Supporting information

Bioinspired thermal reversible adhesive, tough, conductive hydrogels based on nanoclay confined NIPAM polymerization and dopamine modified polypepetide

Xiang Di[a], Chen Hang[a], Yue Xu[a] ,Qiyue Ma[a], Feifan Li[a], Pingchuan Sun[a], Guolin Wu[a,*]

[a]Key Laboratory of Functional Polymer Materials, Institute of Polymer Chemistry, College of Chemistry, Nankai University, Tianjin 300071, PR China.

E-mail: guolinwu@nankai.edu.cn; Fax: +86 22 23502749; Tel: +86 22 23507746

Table S1. The compositions of different hydrogels

Hydrogel	PDAEA/NIPAM (wt.%)	Laponite/Water (wt.%)	NIPAM (g)	KPS (mg)	TEMED (uL)	Water (mL)
PNIPAM-clay	0	2.5	0.5	10	10	5
		5	0.5	10	10	5
		7.5	0.5	10	10	5
		10	0.5	10	10	5
PNIPAM-Clay-PDAEA	1	2.5	0.5	10	10	5
		5	0.5	10	10	5
		7.5	0.5	10	10	5
		10	0.5	10	10	5
PNIPAM-Clay-PDAEA	3	2.5	0.5	10	10	5
		5	0.5	10	10	5
		7.5	0.5	10	10	5
		10	0.5	10	10	5

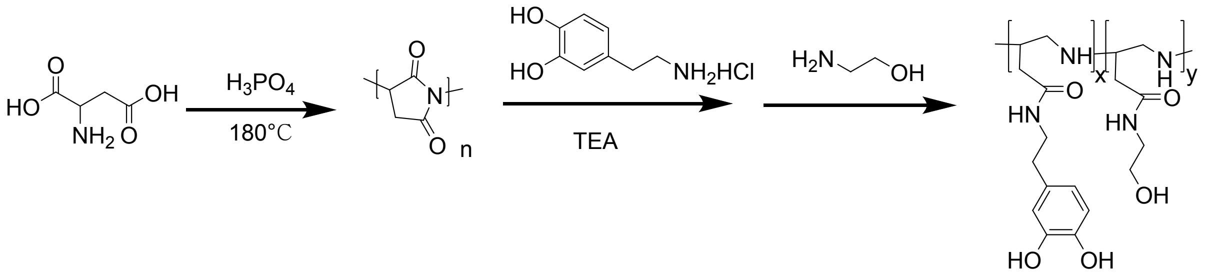

PSI

PDAEA

Figure S1. Synthetic route of dopamine-conjugated PDAEA.

As shown in Figure S1, the polyaspartamide derivatives (PDAEA) were synthesized via the aminolysis reactions. Dopamine, the important role of adhesiveness, was grafted into PSI. Because of the sterichindrance of benzene ring, succinimide ring cannot be totally opened by dopamine. So the rest of succinimide ring was further reacted with ethanolamine to prepare the PDAEA.

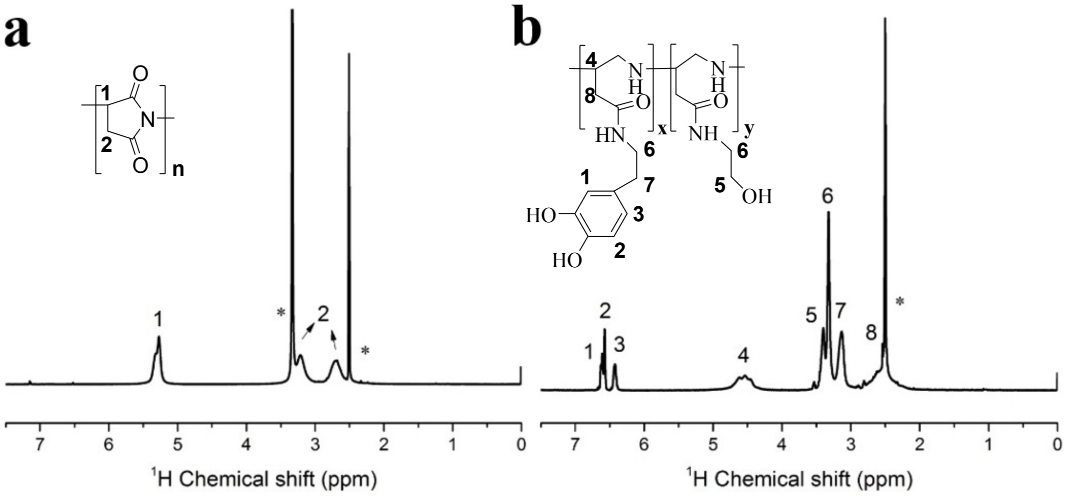

Figure S2. ^{1}H NMR spectra of PSI (a) in DMSO-d_6 and PDAEA (b) in DMSO-d_6.

The structures and compositions of PSI and PDAEA were characterized by ^{1}H NMR spectroscopy in Figure S2. The disappearance of the methane proton (at 5.30 ppm) of the initial succinimide ring and the appearance of the methylene (at 4.70 ppm) of the PDAEA indicated that the methylene aminolysis reactions of PSI. The three peaks at round 6.50 ppm were assigned to the aromatic protons of the dopamine phenyl groups. The dopamine grafting degree is approximately 66% through comparing the 3.20 ppm to 4.70 ppm peaks according to the equation.

$$Grafting\ degree\ of\ dopamine\ (\%) = \frac{The\ intergral\ area\ of\ peak\ 7}{(The\ intergral\ area\ of\ peak\ 4) \times 2} \times 100\%$$

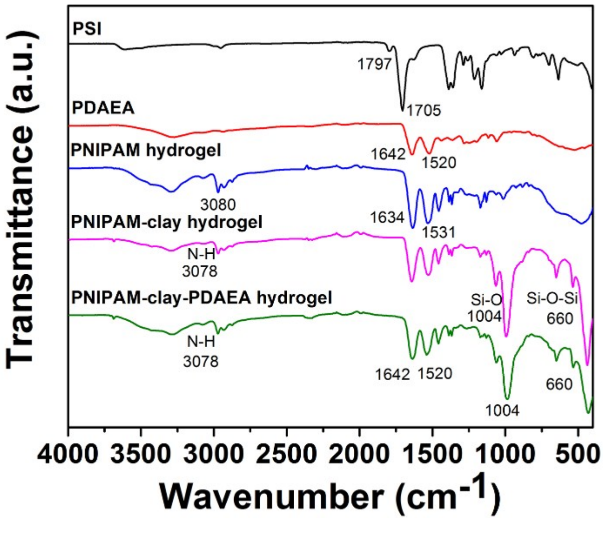

Figure S3. FT-IR spectra of PSI, PDAEA, PNIPAM, PNIPAM-clay and PNIPAM-clay-PDAEA hydrogel.

Figure S3 shows the FT-IR transmittance spectra of PSI, PDAEA, PNIPAM, PNIPAM-clay and PNIPAM-clay-PDAEA hydrogel. The characteristic absorption bands at 1797 cm^{-1} and 1705 cm^{-1} of PSI were attributed to the imide ring. The appearance of new bands around 1642 cm^{-1} and 1520 cm^{-1} of amide further confirm the aminolysis reactions of PSI. As a result, NMR and FT-IR analyses suggest that dopamine was successfully grafted onto the backbone of polyaspartamide. For PNIPAM hydrogel, 1531 and 1634 cm^{-1} peaks were the typical absorption peaks for the N-H bending and C=O stretching, respectively. For PNIPAM-clay hydrogel, the peaks at 1004 and 660 cm^{-1} were attributed to clay (Si-O and Si-O-Si). Besides, all of the PDAEA and PNIPAM-clay characteristic peaks could be observed in the spectrum of PNIPAM-clay-PDAEA hydrogel.

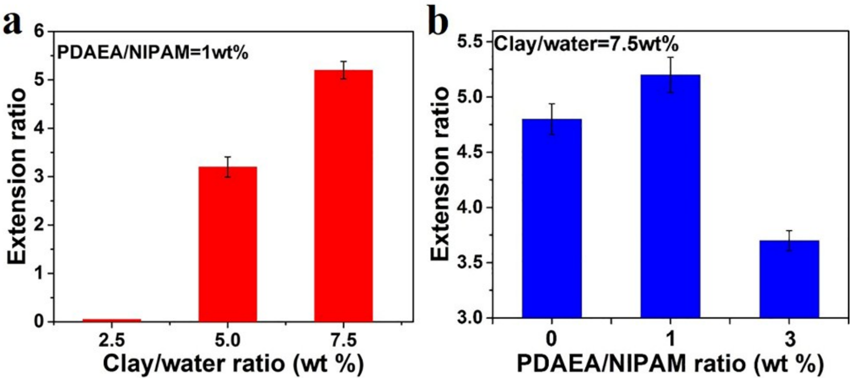

Figure S4. The effect of PDAEA and clay contents on the extension ratio of different hydrogels.

As shown in figure S4, the extension ratio increased with clay content and reached the maximum at the ratio of 7.5wt % at the PDAEA/NIPAM weight ratio was 1wt %. It should be noted that excessive PDAEA could hinder the polymerization of the monomer and cause a decrease in mechanical strength. Therefore, we performed the following characterization at the weight ratio of clay/water, PDAEA/NIPAM of 7.5wt%, 1wt% respectively.

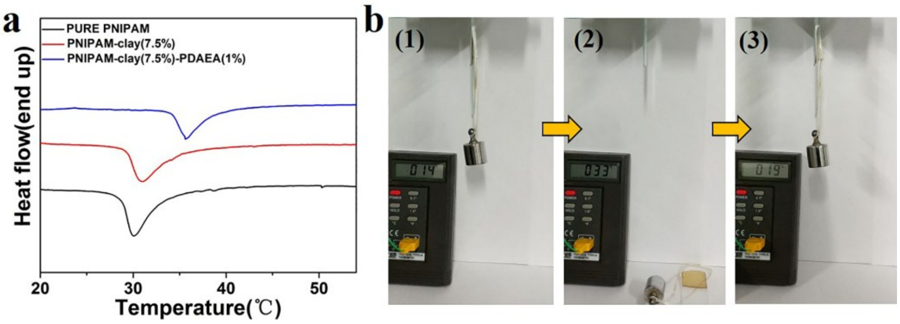

Figure S5. (a) The volume phase transition temperature (VPTT) of different hydrogels. (b) Thermally reversible adhesiveness of PNIPAM-clay (7.5%)-PDAEA (1%) hydrogel.

To investigate the effect of temperature on the adhesiveness of the hydrogels, DSC test was performed to confirm the VPTT of different hydrogels in Figure S5a. The results showed that the VPTT of PNIPAM-clay (7.5%) hydrogel was slight higher pure PNIPAM hydrogel. The addition of PDAEA chains would increase the VPTT to 35.5 ℃, which was ascribed to the hydrogen bonding between PDAEA chains with hydrogel network.

Thermally reversible adhesiveness was shown in Figure S5b, 100g load tightly adhered to the glass (14 ℃), and then the adhesiveness gradually weaken and the load would slide slowly as the temperature rose to VPTT. When turned off the heating, the adhesive strength would recover to its original state.

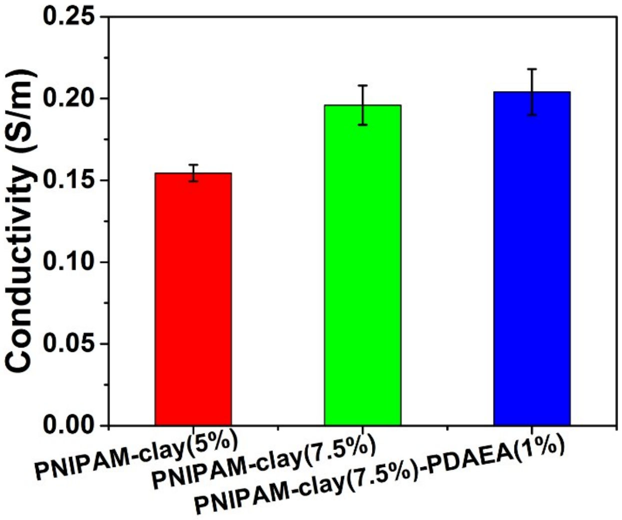

Figure S6. Electrical conductivities of different hydrogels.

The hydrogels provided a water-rich environment for freely moving charges in the network system. The increasing number of ions in the clay enhanced hydrogel conductivity. Besides, the addition of PDAEA chains also improved the conductivity indicating the uniform porous network facilitates the free movement of ions.

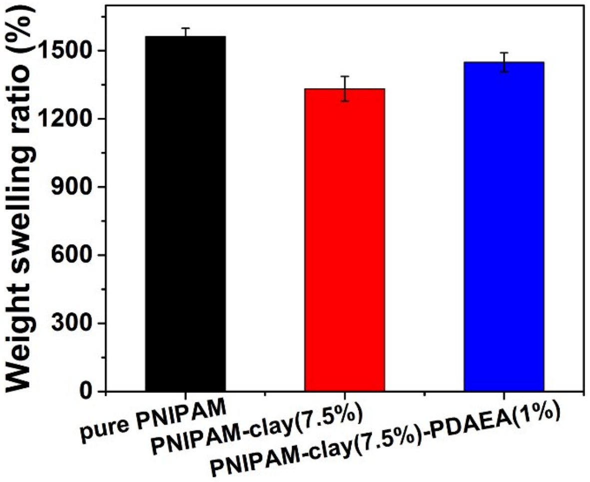

Figure S7. Weight swelling weight ratio of different hydrogels.

The addition of hydrophilic polymer chains PDAEA increased the weight swelling ratio of PNIPAM-clay (7.5%)-PDAEA (1%) hydrogel compared to physical PNIPAM-clay (7.5%) hydrogel.

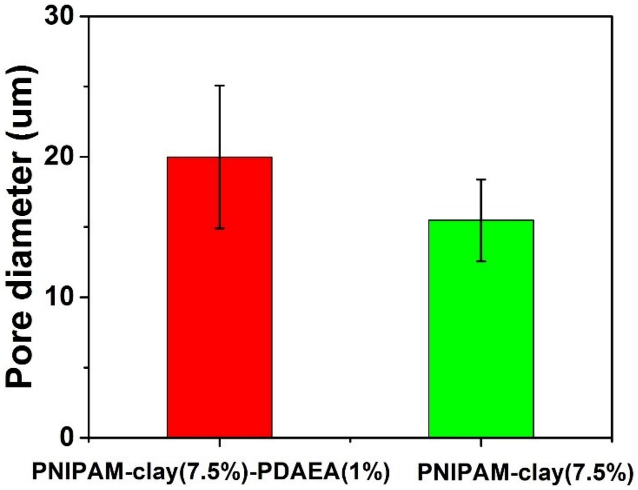

Figure S8. Pore size of different hydrogels.

The average pore diameter of PNIPAM-clay(7.5%)-PDAEA(1%) and PNIPAM-clay(7.5%) hydrogel was 20 μm and 15 μm, respectively. The pore diameter of PNIPAM-clay(7.5%)-PDAEA(1%) hydrogel was bigger than PNIPAM-clay(7.5%)sample, due to the the addition of hydrophilic polymeric chains (PDAEA), which was consistent with the swelling behavior of hydrogels (Figure S7).